https://doi.org/10.5194/essd-2026-422
Preprint. Discussion started: 7 September 2026

Open Access Earth System Science Data Discussions

A European forest disturbance database for robust area estimation and map validation

Cornelius Senf[1], Felix Wieland-Glasmann[1], Katja Kowalski[1], Benjamin Jakimow[2], Anne-Katrin Behrens[1], Veronika Egger[1], Pia Ermert[1], Jonas Hänle[1], Marleen Hanzig[1], Jana Heinrich[1], Antonia Hostlowsky[1], Noah B. Maurer[1], Anabel Onay[1], Moritz Rachfahl[1], Klara Voggeneder[1], & Alba Viana-Soto[1]

[1] Technical University of Munich, School of Life Sciences, Earth Observation for Ecosystem Management, Freising, Germany
[2] Humboldt-University of Berlin, Department of Geography, Earth Observation Lab, Unter den Linden 6, 10099 Berlin, Germany

Correspondence to: Cornelius Senf (cornelius.senf@tum.de)

Abstract. Europe's forests play a critical role as carbon sink, timber production and for the societal well-being, yet their capacity to maintain these functions is increasingly threatened by increasing disturbance rates and a growing demand for wood. Reliable data on disturbance-induced tree cover change are essential to address the challenges faces by Europe's forests. Existing Earth Observation-based products, however, have largely unquantified uncertainties, limiting their potential for robust estimation and reporting. Robust estimation of tree cover change rates and trends, as well as of map uncertainties, requires reference data on tree cover change, covering all of Europe using a probabilistic sample and a harmonized response design. Here, we address this gap by developing a new database of forest disturbances for Europe, based on consistent manual interpretation of satellite imagery from the Landsat archive. Our database covers 35,000 sites across 35 countries, with each site being a 900 m^2 square corresponding to a Landsat pixel, yielding a total of 1,365,000 individual site-year observations. Interpretation was done over the period 1985 to 2023 by trained interpreters, who – for each site-year combination – determined whether a disturbance occurred or not. Disturbances were thereby defined as tree cover loss detectable at a spatial resolution of 900 m^2, caused by either human activity (i.e. harvest), natural disturbances (e.g. bark beetle, fire, wind, avalanches, flooding, etc.) or both (e.g. bark beetle with following salvage logging). Using our database, we exemplify the value of manually interpreted reference data by deriving robust sample-based estimates of disturbance rates and trends. We further compare our sample-based estimates to state-of-the art map-based estimates, highlighting uncertainties in relying solely on Earth observation. Our results underscore the need for consistent, transparent, and independent reference data for understanding disturbance change in Europe and for validation and uncertainty quantification in Earth observation data.

1 Introduction

There is accumulating evidence that forest disturbances have increased across Europe's forests in recent decades (Senf et al., 2018, 2021). While approximately 80% of all disturbances are planned human interventions (i.e. timber harvest), around one

https://doi.org/10.5194/essd-2026-422
Preprint. Discussion started: 7 September 2026

fifth of recorded canopy openings are related to natural agents such as wildfires, windstorms or insect outbreaks (Seidl and Senf, 2024). Such natural disturbances have significantly increased in recent years (Patacca et al., 2023), with climate-sensitive disturbances (i.e. wildfires and insect outbreaks) being fuelled by climate extremes (Senf et al., 2020) and past land use decisions (Seidl et al., 2011). There are rising concerns about the socioeconomic and ecological impacts of increasing disturbance, as both the demand for wood (Lerink et al., 2023; Migliavacca et al., 2025) and the occurrence of climate-sensitive disturbances are expected to increase (Seidl et al., 2014). Increasing disturbances can alter forest demography (Senf et al., 2021), reduce the carbon storage potential of forests (Seidl et al., 2014), their economic value (Mohr et al., 2025) and put other important forest ecosystem services at risk (Lecina-Diaz et al., 2024). To prepare Europe's forests for a world with more disturbances, a better understanding of disturbance change is required.

Remote sensing has become a major tool for understanding disturbance change (Fassnacht et al., 2014; Lechner et al., 2020; McDowell et al., 2015; Senf, 2022), with several continental to global tree cover loss products being available (Hansen et al., 2013; Hermosilla et al., 2015; Senf and Seidl, 2021; Turubanova et al., 2023; Viana-Soto and Senf, 2025). Among these products, several have been developed specifically for Europe (Senf and Seidl, 2021; Turubanova et al., 2023; Viana-Soto and Senf, 2025). Such tree cover loss products – often simply referred to as "disturbance maps" – map land cover transitions from treed to non-treed, where the loss of trees is either caused by human or natural causes. While such disturbance maps deliver detailed insights into where and when tree cover loss is occurring, estimation of disturbed area and disturbance changes remains challenging. First, all remote sensing maps have errors, and simply counting pixels flagged as tree cover loss can lead to over- or underestimation of disturbed area, depending on whether commission errors (mapping change that is not real) or omission errors (not mapping change that is real) prevail (Olofsson et al., 2014). Second, errors in disturbance maps might change through time, which makes estimation of trends even more challenging. Image density, quality and properties have changed in time, which can result in variable errors, with data availability and quality being generally higher in more recent years (Frantz et al., 2023). Depending on how tree cover loss is detected, more recent changes might also spatially overlap with past tree cover loss and "mask" them, further introducing temporal bias.

To overcome the above-mentioned challenges in quantifying disturbance area and change from remote sensing maps, sample-based approaches have long been suggested in the literature (Cohen et al., 2017, 2016; Olofsson et al., 2014; Stehman, 2000, 2009; Stehman and Foody, 2019). With sample-based approaches, the remote sensing map serves as stratum for selecting locations for more detailed analysis (Olofsson et al., 2013). Using a disturbance map as stratum allows for selecting locations for interpretation with more accurate methods, such as analysis of aerial imagery, field visits, or manual interpretation of satellite time series (Cohen et al., 2010, 2016; Pickens et al., 2020; Senf et al., 2018; Turubanova et al., 2023). Doing so enables an efficient and precise estimation of disturbance area from a relatively small sample, despite disturbances being of low abundance in the underlying population. As the sample will be biased with respect to the underlying population, however, unbiased estimators must be used that incorporate the map strata as weights (Olofsson et al., 2014). A targeted sample not only allows for unbiased and precise estimation of disturbance areas, but also for reliable assessments of map accuracies (Stehman and Foody, 2019). While sample-based estimates can be considered the gold-standard for estimating disturbance area from

https://doi.org/10.5194/essd-2026-422
Preprint. Discussion started: 7 September 2026

remote sensing data, they are ignored in many scientific studies. One reason for this is the wide availability of remote sensing-based maps and novel processing tools that allow for easy creation of map products (Gorelick et al., 2017). Interpreting a sample with more detailed methods, in turn, is often laborious and time-consuming. This often incautious reliance on remote sensing-based maps has led to inconclusiveness about disturbance change in Europe (Breidenbach et al., 2020; Ceccherini et al., 2020, 2022; Palahí et al., 2021; Wernick et al., 2021). Solving this knowledge gap requires an investment into collecting reliable reference data on disturbances across all Europe's forest land, allowing for robust estimation of disturbance area and change.

We here provide a consistent database on forest disturbance occurrence covering 35,000 sites across 35 countries in Europe and four decades (1985 to 2023), resulting in 1,365,000 individual site-year observations. A site thereby refers to a square of 900 m^2 and a disturbance is following defined as any tree cover loss detectable at 900 m^2. This size was chosen, because interpretation is based on Landsat satellite data, the longest achieve of freely available optical satellite data, for which we present a new open-source interpretation tool with corresponding protocols. Based on our database, we exemplify how the data can be used to estimate disturbance rates, trends and total disturbance area at national and regional scales. Our database allows for the most up-to-date and accurate quantification of disturbance and disturbance change for Europe's forest, serving as benchmark for future studies.

2 Data collection

2.1 Study area

Our study focused on 35 countries in continental Europe, covering a total forested area of approximately 2.2 million km^2. These countries represent a diversity of boreal, temperate and Mediterranean forest ecosystems, spanning from lowland to alpine and from maritime to continental conditions. The study region also encompasses a broad range of forest disturbance regimes and management systems, with windthrow, bark beetle and fire being the most important natural agents of stand-replacing disturbances in Europe (Patacca et al., 2023); and clear-cut harvest the most important stand-replacing management intervention (Suvanto et al., 2023).

2.2 Landsat data

Our data processing pipeline is similar to Viana-Soto & Senf, 2025 and we here only summarize the salient details. We downloaded all available Landsat 4–9 Collection-2 images from 1984 to 2024 with less than 80 % cloud cover. To minimize seasonal effects, only scenes from the main growing period (June to September) were used. In total, 160,858 images were downloaded from the United States Geological Survey. Images were corrected to surface reflectance using the FORCE processing framework (v3.7.10; Frantz, 2019) and organized into a tiled data cube (150 × 150 km^2 per tile). Pre-processing steps included atmospheric and topographic correction, bidirectional normalization, and automated cloud and shadow detection (Frantz, 2019; Roy et al., 2016; Zhu and Woodcock, 2012). We then produced yearly, cloud-free image composites for the full

https://doi.org/10.5194/essd-2026-422
Preprint. Discussion started: 7 September 2026

region using the Best Available Pixel approach (Griffiths et al., 2013). For each pixel, the best available observation was chosen using a parametric weighting scheme that prioritized minimal cloud and haze interference and proximity to a reference date (1st August). This approach has been shown to yield radiometrically consistent mosaics well-suited for disturbance monitoring (Francini et al., 2023). We filled the remaining data gaps (roughly 10% of total area on average) with a linear gap-filling algorithm, extrapolating spectral values from the previous year imagery.

2.3 Sampling design

We applied a stratified equalized sampling design, selecting 1,000 sites per country within forests, resulting in a total of 35,000 sites (Figure 1). A site thereby represents a square of 900 m^2 (30×30 m^2), corresponding to a Landsat pixel. The location of each site equals exactly the centre of the square/Landsat pixel. We chose equal sample sizes per country to allow for similar precision in area estimation per country, with countries being the primary reporting unit in Europe. Forests were identified using an existing forest land use map (Viana-Soto and Senf, 2025), defining forest land use as pixels containing 50 % or greater tree cover at some time during the time series. We further allocated half of the sites to areas disturbed between 1985 and 2023 and the other half to areas undisturbed in the same time period, using an up-to-date disturbance map (Viana-Soto and Senf, 2025). Stratification was done to increase sampling efficiency, because disturbances are rare events and a random sample without stratification might result in only few disturbances included in the sample. For both stratifications – among countries and disturbed/non-disturbed forest area within countries – we provide stratum weights in Table 1. Stratum weights were derived from the proportion of each countries forest area among total forest area in Europe (to account for stratification among countries), as well as from the proportion of disturbed/non-disturbed forest within each country (to account for the stratification among disturbed/non-disturbed forest within countries). We finally matched our sampling design to include sites already interpreted in earlier studies (Senf et al., 2018, 2021). For doing so, we first selected sites from the existing sample according to our stratification (resulting in variable number of sites per stratum), and following filled up the sample to match our sampling design (i.e. 500 sites per stratum/country). From the existing sample, we identified all sites that had a record of disturbance, plus all sites without record of disturbance but a disturbance identified in the disturbance maps used for stratification. That way, we identified sites that needed to be reinterpreted to match interpretation protocols and data quality between the existing and new sites. For all existing sites without any record of disturbance in both, the manual interpretation and the disturbance map, we assumed no tree cover loss to be present, and we refrained from re-interpretation. This applied to 3,556 sites (10.2 % of all samples).

https://doi.org/10.5194/essd-2026-422
Preprint. Discussion started: 7 September 2026

Open Access Earth System Science Data Discussions

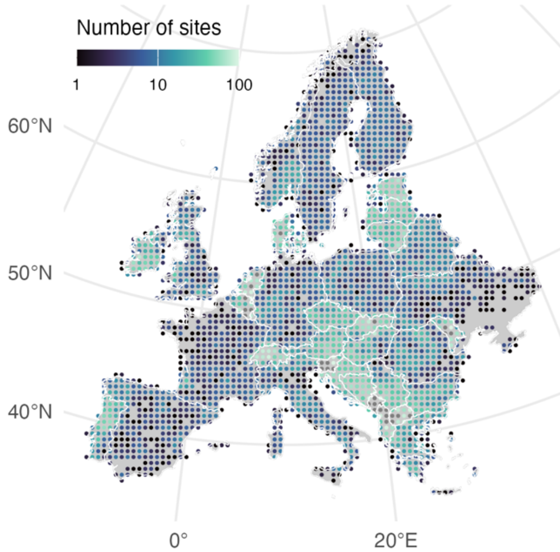

Figure 1: Sampling density aggregated to a 50 x 50 km^2 grid with colours indicating number of sites. In grey areas there were no samples allocated.

Table 1: Overview of the sample, with country-wise forest area and sampling density, as well as stratum weights. Stratum weights refer to the stratification by disturbance/no disturbance within each country, with stratum weights representing the proportion of disturbed/non-disturbed forest for each country; as well as to the stratification by country, with stratum weights representing the proportion of each countries forest area among total forest area in Europe. The former stratum weight can be used to calculate unbiased estimates at the country level (i.e. correcting for the stratification among disturbed/non-disturbed forest within a country), whereas the latter can be used to calculate unbiased estimates across countries (i.e. correcting for the stratification among countries).

Country	Forest area (km^2)	Samples per 100 km^2 forest	Stratum weights		
			Disturbance	No disturbance	Forest area
Albania	9,148	10.93	0.21	0.79	0.00
Austria	44,980	2.22	0.23	0.77	0.02
Belarus	96,192	1.04	0.26	0.74	0.04
Belgium	8,484	11.79	0.28	0.72	0.00
Bosnia and Herzegovina	30,054	3.33	0.16	0.84	0.01
Bulgaria	46,152	2.17	0.21	0.79	0.02
Croatia	27,461	3.64	0.18	0.82	0.01
Czechia	32,721	3.06	0.30	0.70	0.02
Denmark	6,788	14.73	0.34	0.66	0.00
Estonia	28,663	3.49	0.35	0.65	0.01
Finland	245,919	0.41	0.39	0.61	0.11
France	177,107	0.56	0.22	0.78	0.08
Germany	122,334	0.82	0.22	0.78	0.06
Greece	42,472	2.35	0.18	0.82	0.02
Hungary	22,216	4.50	0.33	0.67	0.01
Ireland	7,280	13.74	0.30	0.70	0.00
Italy	94,920	1.05	0.20	0.80	0.04
Latvia	38,783	2.58	0.40	0.60	0.02
Lithuania	24,327	4.11	0.30	0.70	0.01
Macedonia	11,491	8.70	0.21	0.79	0.01

https://doi.org/10.5194/essd-2026-422
Preprint. Discussion started: 7 September 2026

Moldova	3,114	32.11	0.18	0.82	0.00
Montenegro	8,814	11.35	0.21	0.79	0.00
Netherlands	5,733	17.44	0.27	0.73	0.00
Norway	115,255	0.87	0.23	0.77	0.05
Poland	111,500	0.90	0.26	0.74	0.05
Portugal	30,876	3.24	0.61	0.39	0.01
Romania	88,387	1.13	0.19	0.81	0.04
Serbia	38,549	2.59	0.22	0.78	0.02
Slovakia	24,679	4.05	0.19	0.81	0.01
Slovenia	13,380	7.47	0.12	0.88	0.01
Spain	149,084	0.67	0.30	0.70	0.07
Sweden	307,208	0.33	0.39	0.61	0.14
Switzerland	14,919	6.70	0.15	0.85	0.01
Ukraine	104,361	0.96	0.21	0.79	0.05
United Kingdom	24,756	4.04	0.23	0.77	0.01

2.4 Interpretation tool

To support the interpretation of Landsat time series for detecting changes in forest canopy, we adapted an existing interpretation tool implemented in the open-source geo-information system QGIS (Jakimow et al., 2020) to match our approach. The tool allows for direct visualization of spectral trajectories at the pixel level and image chips of the surrounding area in variable band combinations/spectral indices at selected sites (see Figure 2). Interpretation results can be added directly to an underlying attribute table. The tool is similar to other interpretation tools presented in the literature (Cohen et al., 2010) but fully integrated into the open-source QGIS environment (EO Time Series Viewer, Version 2.1; https://plugins.qgis.org/plugins/timeseriesviewerplugin/).

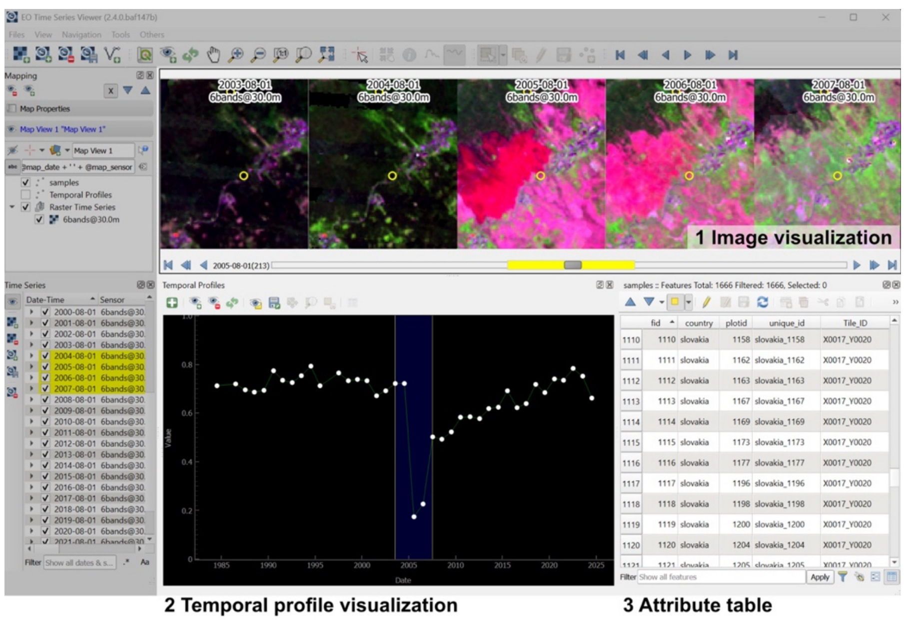

Figure 2: Example of a sample site in Slovakia visualized in the interpretation tool.

2.5 Response design

All sites were interpreted by a total of eleven trained interpreters. The goal of the manual interpretation was to determine if and in what year a tree cover loss happened at the selected site, i.e. a square of 900 m^2 corresponding to a Landsat pixel, between 1985 and 2023. We couldn't interpret the years 1984 and 2024, despite satellite imagery being available, as one year leading/following is needed for robust interpretation. A tree cover loss was defined as a reduction of the top forest canopy by more than 50 %. To identify such losses, the experts made use of different spectral band combinations for visualizing the Landsat composites, different spectral indices, and the spectral band/index time series (see Figure 2). Tree cover loss is usually identifiable by a sudden drop in common spectral indices at the site/pixel level, but we cross-checked each spectral index time series with image chips of the region to ensure that spectral deviations were not caused by, e.g., sensor noise, phenological variation, failed atmospheric correction, or remnant clouds. The final decision was further corroborated by cross-checking with high-resolution, historic Google Earth imagery. When discrepancies occurred between the interpretation and Google Earth imagery, priority was always given to the Landsat time series. Pixels were considered undisturbed when no tree cover loss could be detected, i.e. the Normalised Burn Ratio (NBR) time series showed no abrupt decline, fluctuations could be explained by noise, or when an apparent decrease was followed by unrealistically rapid recovery (i.e. within a year). In these cases, Google Earth imagery was used, where available, to confirm whether fast recovery reflected shrub regrowth or sparse tree cover. Pixels were also classified as undisturbed when observed declines could be attributed to mixed pixel effects or surrounding land use changes (e.g. grassland/agriculture), or when < 50% of the crown cover was removed, such as in partial harvests confined to a pixel corner. If a tree cover loss was detected, we recorded the start year and the end year. The start year was defined as the year with the first visible spectral drop. The end year was defined as the year prior to the continuous recovery, e.g. represented by the increase of NBR following a disturbance, marking the onset of recovery. While most events only last one year, in some cases (e.g. unmanaged bark beetle infestation) a more gradual declines of up to 5 years were observed. Missing data due to clouds or other gaps were addressed by considering adjacent observations in the time series. In all cases, decisions were made conservatively and restricted to information that could be substantiated by available data. Where uncertainty existed in determining disturbance years, later years were assigned for disturbance onset and earlier years for disturbance end.

2.6 Quality assessment

Human interpretation is subject to errors. We therefore assigned a confidence flag to each interpretation, generated from cross-checking the manual interpretation with year-to-year changes in NBR. As disturbances are associated with significant negative changes in NBR (see Figure 3), we flagged all disturbance observations with NBR changes > -850 and all non-disturbance observations with NBR changes <= -850 as low confidence. All other cases, a disturbance observation with NBR changes <= -850 and non-disturbance observations with NBR changes > -850, were flagged as high confidence. We further tested whether manual interpretation was repeatable, that is whether another interpreter would arrive at the same label when reinterpreting a

https://doi.org/10.5194/essd-2026-422
Preprint. Discussion started: 7 September 2026

Open Access Earth System Science Data Discussions

site. We therefore randomly sub-sampled 100 sites for reinterpretation. This reinterpretation was done using the same response design (see Section 2.5), but jointly by two interpreters to discuss difficult cases. We then compared the label in the initial database to the reinterpretation.

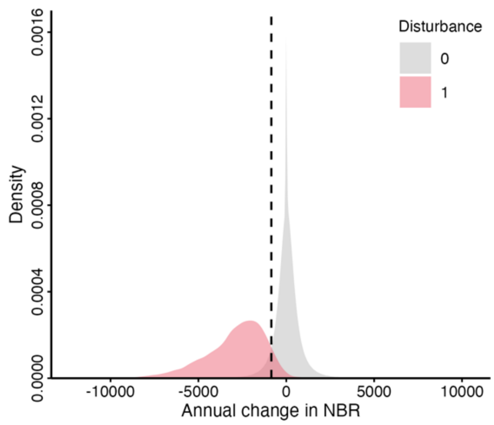

Figure 3: Year-to-year changes in Normalized Burn Ratio (NBR) summarized for entries with a disturbance record and without a disturbance record. The threshold of -850 NBR change was chosen to separate low and high confidence labels.

2.7 Final database

The database is distributed as long-format table with 14 attributes. Each sample location has a unique id (attribute: *unique_id*) based on the country name (attribute: *country*) and a running number. Each sample location has unique x and y coordinates (attribute: *x*/*y*), recorded in EPSG:3035 (ETRS89-extended / LAEA Europe) coordinate reference system. There is further information on the year (attribute: *year*) and stratum (attribute: *stratum*), with years being continuous years from 1985 to 2023 and stratum being either 0 (undisturbed forest) or 1 (disturbed forest). In total, there are 35 countries, 39 years and two strata, with 500 sampling location per stratum, resulting in a total of 1,365,000 data entries. Besides the basic information on each sampling location, there are five attributes on disturbances: *disturbance*, *rank*, *start*, *end* and *length*. The attribute *disturbance* is a binary label indicating the presence (1) or absence (0) of a disturbance event for each site-year combination. If no disturbance was present, all following attributes are set to NA. In case a disturbance was present, *rank* gives the rank of the disturbance within the sample location, starting from first to last; *start* gives the start year of the disturbance, which is equal to the year of the record; *end* gives the end date of the disturbance; and *length* gives the length of the disturbance (*end* - *start*). Finally, the certainty flag is stored in *confidence*, indicating either low or high interpretation certainty. Additinally, we provide NBR values of each record derived from the underlying Landsat data (*nbr*), as well as NBR change to the previous year used for constructing the confidence flag (*nbr_change*). In total, we recorded 1,350,776 entries without disturbance and 14,224 entries with disturbance. Aggregating the long-format table to the site level yields a total of 35,000 sites, with 12,475 sites

https://doi.org/10.5194/essd-2026-422
Preprint. Discussion started: 7 September 2026

having at least one disturbance recorded, of which 10,954 have exactly one and 1521 have more than one disturbance per site. From all 1,350,776 entries, a total of 95,045 (7.0 %) were of low confidence, of which almost all (94,009) were low confidence non-disturbance records.

3 Uncertainties and limitations

Our database presents the largest database on disturbance occurrence across Europe. While valuable for gaining insights into disturbance change (see Section 4), there are uncertainties and limitations that need to be considered when using the database. First, manual interpretation was done by trained interpreters, but interpretation might be subject to errors. While we tried to minimize uncertainty arising from manual interpretation by cross-checking between interpreters and discussing difficult sites among interpreters, there is still a chance that manual interpretation might deviate from the reality observed on ground. This might be particularly true for pixels mixed of disturbed and non-disturbed forest. That said, comparison to on ground information is impossible for historic data and our approach thus presents – up to our knowledge – the most reliable assessing historic disturbances in optical satellite time series (Cohen et al., 2010, 2016; Olofsson et al., 2013; Senf et al., 2018; Tyukavina et al., 2025). We nonetheless performed a consistency check on the final interpreted by checking for reproducibility of the interpretation results (see Section 2.6). We found an overlap of 90 % between the original interpretation and reinterpretation, indicating high reproducibility. Second, there is temporal uncertainty stemming from the annual resolution of the underlying Landsat image database, which can lead to imprecision in assigning the exact year of disturbance. For instance, if a disturbance happens in autumn of one year, it will only be recorded in the next year if annual Landsat data of the disturbance year precede the disturbance event. This happened, for example, with storm Lothar in 1999, which happened in December and is thus recorded in the following year in our database (see peak in 2000 in Figure 5/Western Europe). Third, the spatial resolution of Landsat can mismatch small-scale disturbances and individual tree mortality. While disturbances only affecting parts of a pixel can be detected, the nature of optical satellite data does not allow for detecting tree cover change below the canopy, and small gaps from individual trees below the size of a Landsat pixel (900 m^2) will be missed in the analysis (Senf et al., 2025). Finally, we restricted our sample to an existing forest land use mask (Viana-Soto and Senf, 2025), which can have errors and thus exclude forest areas from the sample. While we assume this error to be small (see Viana-Soto and Senf 2025 for a validation of the forest land use mask), the estimates derived from the sample are only valid for the corresponding forest land included in the mask.

4 Application examples

For exemplifying the use of the database, we estimate annual disturbance rates and trends in disturbance rates from the disturbance database. Annual disturbance rates were estimated from the sample using a Bayesian hierarchical binomial model (Senf et al. 2018). With such a model, annual disturbance rates are treated as a series of binary outcomes across sites within

https://doi.org/10.5194/essd-2026-422
Preprint. Discussion started: 7 September 2026

each country, with the annual disturbance rate corresponding to the proportion of sites recording a tree cover loss relative to the total number of sites. We added country as fixed effect accounting for differences in average disturbance rates between countries, whereas year was added as random effect nested within country to account for year-to-year variation. This hierarchical structure corresponds to a partially pooled model that assumes annual disturbance rates to be drawn from an underlying country-specific distribution. This approach regularizes the yearly estimates by shrinking them toward the country-level mean, which reduces the impact of extreme years dominated by exceptional disturbance events (e.g., severe storms or large fire seasons), and it reduces the influence of potential observation or interpretation errors. Joint posteriors for all model parameters were sampled using Monte-Carlo-Markov-Chain methods implemented in Stan (Carpenter et al., 2017). Weakly-informative priors were used for all parameters (Senf et al., 2018) and sampling was done using four chains in parallel, with 1,000 draws per chain. We created separate models for each stratum (i.e. one model for sites in the *disturbed* stratum and one model for sites in the *undisturbed* stratum), and joint estimates were subsequently created by calculating weighted means per draw (see Table 1 for sampling weights). This guarantees unbiased estimates despite stratification in the sampling process. Following, we aggregated country-year-specific posteriors to regional units (Northern, Western, Central, Eastern, Southern [west] and Southern [east] Europe), as well as for all of Europe, by averaging per draw, using forest land share as weighting factor (i.e. ensuring consistency with the stratified sampling design). For estimating trends, we used a simple trend estimator (Theil-Sen-Slope), which we calculated for each draw of the posterior. This yields a posterior distribution of trend estimates, allowing us to derive levels of evidence by calculating the proportion of trend estimates above/below zero (i.e. the probability that a country has a positive or negative trend in disturbance rates). Trends were calculated at the national, regional and European level. We finally compared our sample-based estimates with other sample-based estimates (Senf et al., 2018, 2021) and state-of-the-art map-based estimates for Europe (Hansen et al., 2013, 2013; Senf and Seidl, 2021; Viana-Soto and Senf, 2025; Viana-Soto et al. 2026 [unpublished]). Specifically, we compare total disturbance area aggregated to countries.

Across Europe, the average annual disturbance rate was between 0.72 and 0.75 % $yr.^{-1}$ (here reported are the 80% credible interval, i.e. the range between the 10% and 90% quantiles of the joint posterior). Splitting by region, we estimate average disturbance rates to be highest in Southern Europe West (0.98 – 1.08 % $yr.^{-1}$) and Northern Europe (0.79 – 0.88 % $yr.^{-1}$), and lowest in Southern Europe East (0.47 – 0.52 % $yr.^{-1}$) and Central Europe (0.55 – 0.61 % $yr.^{-1}$). Eastern (0.61 – 0.70 % $yr.^{-1}$) and Western Europe (0.64 – 0.76. % $yr.^{-1}$) were close to the European average. At the country level (Figure 4), highest average annual disturbance rates were estimated for Portugal (2.88 – 3.22 % $yr.^{-1}$) and Latvia (0.93 – 1.10 % $yr.^{-1}$), whereas lowest average annual disturbance rates were estimated for Slovenia (0.17 – 0.25 % $yr.^{-1}$) and Romania (0.31 – 0.40 % $yr.^{-1}$).

https://doi.org/10.5194/essd-2026-422
Preprint. Discussion started: 7 September 2026

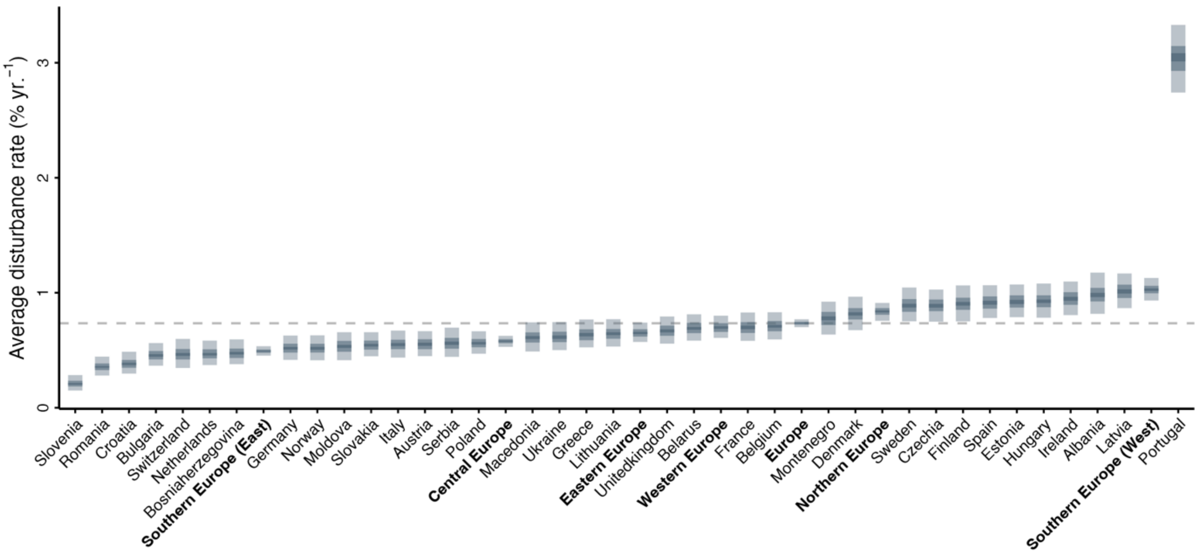

Figure 4: Average annual disturbance rates for 35 European countries, six regions and Europe, estimated from the disturbance database presented in this study. The dashed line shows the European average. Light blue colours show the 80 % credible interval (from the 10 % to the 90 % quantile), middle blue shades the 50 % credible interval (from the 25 % to the 50 % quantile) and the dark blue line the 50 % quantile of the joint posterior distribution.

We record several instances of well-known disturbance events in the European time series of disturbance rates (Figure 5), such as storm Vivian-Wiebke in 1990, storm Lothar in 1999, or recent increases in bark beetle disturbances after the year 2018 (Patacca et al., 2023). Across Europe, the years with highest disturbance rates were 2018 (0.83 – 1.07 % yr.$^{-1}$), 2023 (0.77 – 1.02 % yr.$^{-1}$) and 1990 (0.74 – 0.95 % yr.$^{-1}$; because of storms Vivian and Wiebke in February 1990). Among the ten most severe years, five occurred in the last six years of the time series (2018, 2019, 2021, 2022 and 2023); and since 2018 already three years (2018, 2019 and 2023) showed similarly high disturbance rates as the most extreme year in the three decades before (1990). The strong increase in extreme disturbance years in recent years was, however, not consistent among regions: While Central Europe and Northern Europe followed the overall trend, Eastern and Western Europe had extreme disturbance years less concentrated in the last decade, and Southern Europe showed high year-to-year variation with some extreme fire years standing out in the west (i.e. 1985, 1989, 1994, 2005, 2017 and 2018).

https://doi.org/10.5194/essd-2026-422
Preprint. Discussion started: 7 September 2026

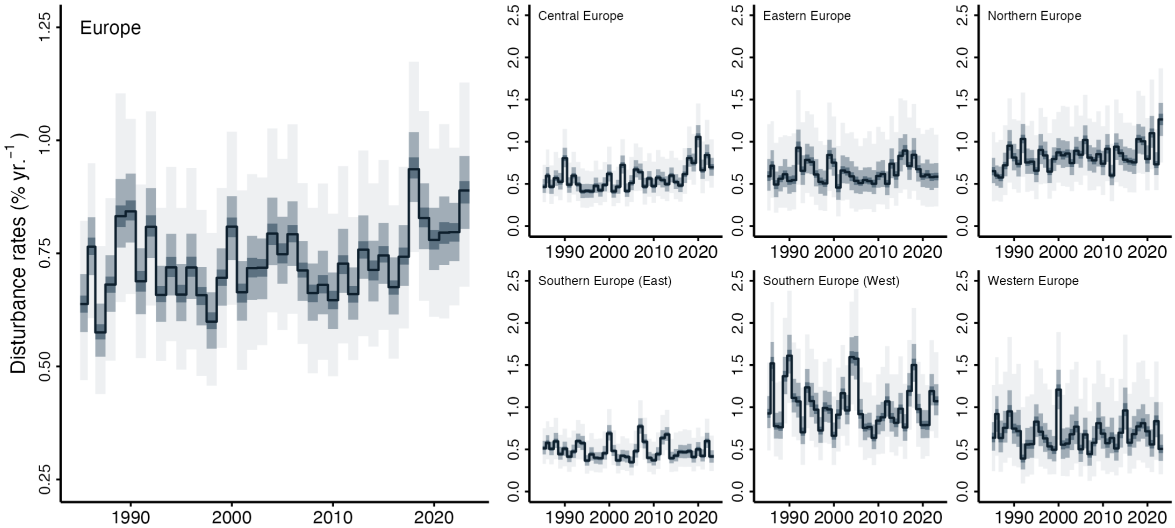

Figure 5: Annual disturbance rates for six regions and Europe, estimated from the disturbance database presented in this study. Light blue colours show the 80 % credible interval (from the 10 % to the 90 % quantile), middle blue shades the 50 % credible interval (from the 25 % to the 50 % quantile) and the dark blue line the 50 % quantile of the joint posterior distribution.

Across Europe, the probability of a positive trend in disturbance rates was p = 0.88, with disturbances increasing by 0.00 – 0.17 % pts. 10 yrs.$^{-1}$ (Figure 6). At regional scales, Northern and Central Europe showed high probabilities of a positive increase in disturbance rates (p = 0.97 and p = 0.99, respectively), with increases of 0.02 – 0.09 % pts. 10 yr.$^{-1}$ for Northern Europe and 0.03 – 0.08) % pts. 10 yr.$^{-1}$ for Central Europe. No strong support of a positive or negative trend was found for Eastern and Western Europe. Southern Europe (east and west), however, showed a moderate probability (p = 0.72 [east] and p = 0.79 [west]) for decreasing disturbance rates at -0.03 – 0.01 % pts. 10 yr.$^{-1}$ and -0.07 – 0.01 % pts. 10 yr.$^{-1}$, respectively. At the country level, 11 out of the 35 countries had a probability p > 0.8 for increasing disturbances, with strongest increases observed for Latvia (0.18 – 0.31 % pts. 10 yr.$^{-1}$; p = 1.00) and Estonia (0.15 – 0.28 % pts. 10 yr.$^{-1}$; p = 1.00). Six out of the 35 countries showed evidence (p > 0.8) for a negative trend, with strongest decrease observed in Albania (-0.15 – -0.01 % pts. 10 yr.$^{-1}$; p = 0.93) and Spain (-0.12 – 0.01 % pts. 10 yr.$^{-1}$; p = 0.88).

https://doi.org/10.5194/essd-2026-422
Preprint. Discussion started: 7 September 2026

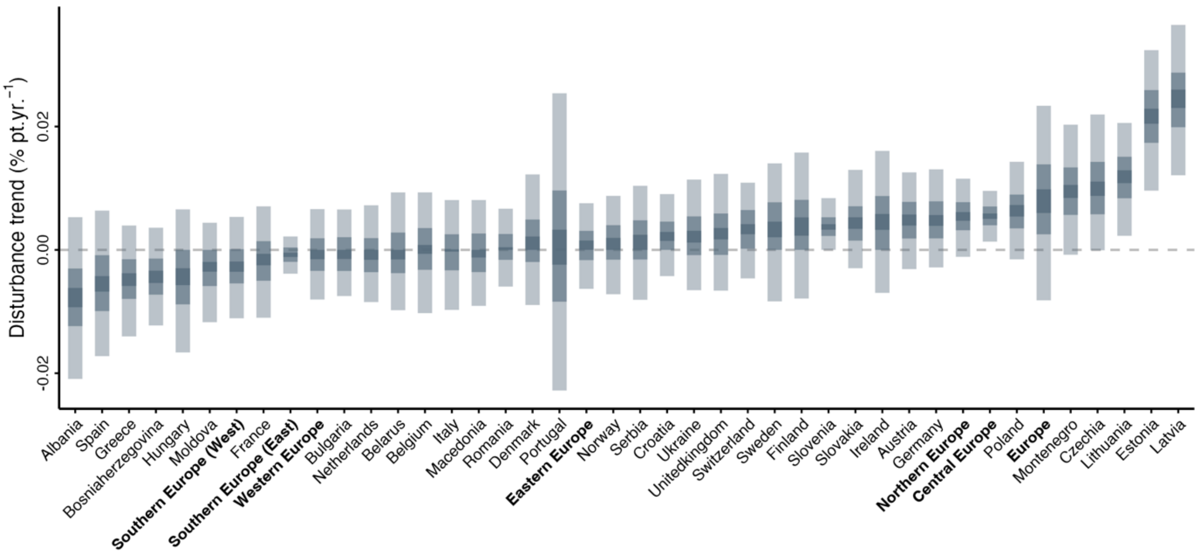

Figure 6: Linear trends in disturbance rates based on Theil-Sen slopes for 35 countries in Europe, six regions and Europe, estimated from the disturbance database presented in this study. Light blue colours show the 80 % credible interval (from the 10 % to the 90 % quantile), middle blue shades the 50 % credible interval (from the 25 % to the 50 % quantile) and the dark blue line the 50 % quantile of the joint posterior distribution.

Comparing our sample-based estimates of the total area disturbed per country to other sample-based and map-based estimates showed high agreement in the ranking of countries, but variable mean absolute errors and biases (Figure 7). We here note that we standardized the analysis timeframe to the smallest overlapping period among all products, which was 2001 to 2018. For this period, we estimate a total area disturbed of 26.5 million ha from our sample, 38.2 million ha from the sample of Senf et al. 2021 (+41 %), 17.5 million ha from the map of Hansen et al. 2013 (-35 % compared to our sample-based estimate), 21.1 million ha from the map of Senf and Seidl 2021 (-22 %), 19.7 million ha from the map of Turubanova et al. 2023 (-27 %), 36.5 million ha from the map of Viana-Soto and Senf 2015 (+35 %), and 29.1 million ha from the map of Viana-Soto et al. 2026 (+8 %). Two of the five map products showed moderate to strong negative bias (Hansen et al. 2013, Senf and Seidl 2021 and Turubanova et al. 2023), indicating overall higher omission than commission errors. One map product (Viana-Soto & Senf 2025) showed strong positive bias, indicating higher commission than omission errors. Only one map product had a bias < 1000 km^2 (Viana-Soto et al. 2026), indicating more balanced commission and omission errors. Mean absolute errors ranged from 1656 km^2 (Turubanova et al. 2023) to 3207 km^2 (Viana-Soto and Senf 2025), indicating a relative error (relative to the average sample-based disturbance area) of 0.2 to 0.39 %, and thus low for all map products. That said, errors were often larger in countries with fewer disturbances, thus leading to relatively larger errors in those countries.

https://doi.org/10.5194/essd-2026-422
Preprint. Discussion started: 7 September 2026

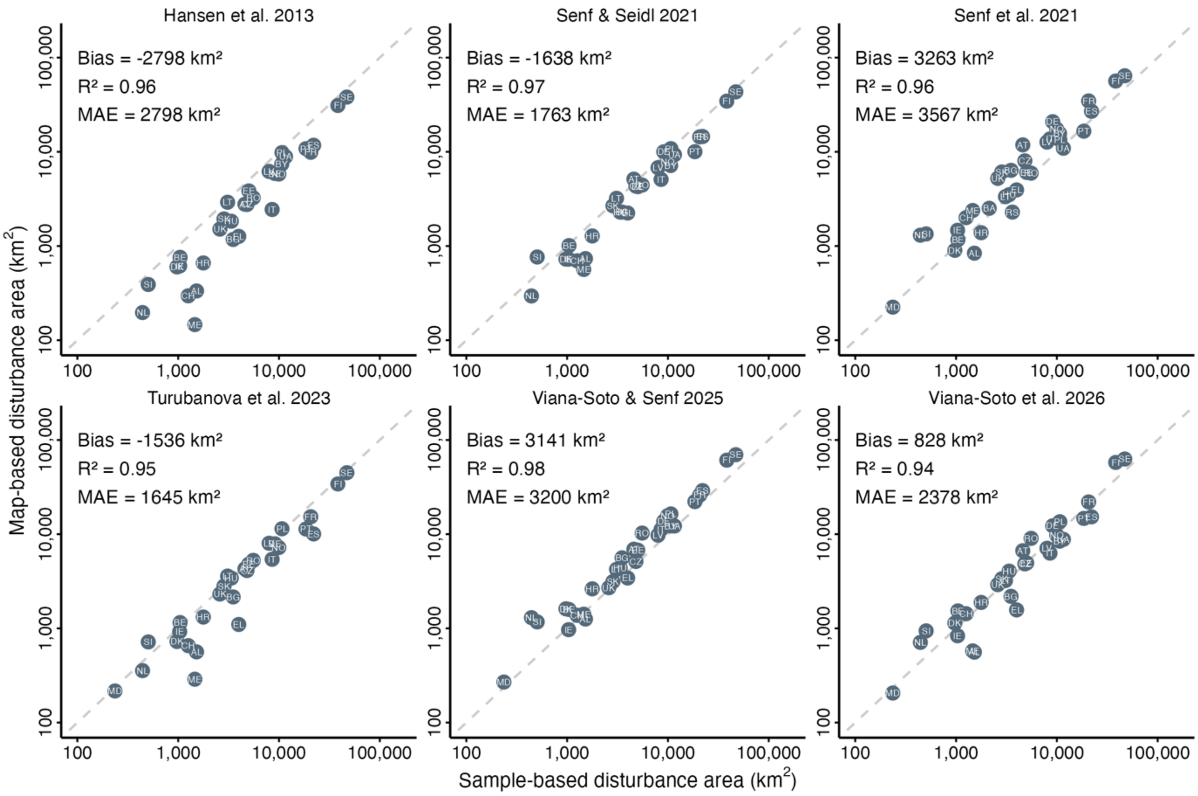

Figure 7: Comparison of our sample-based estimate of country-level total disturbance area to other sample-based estimates (Senf et al. 2021) and map-based estimates (Hansen et al. 2013, Senf and Seidl 2021, Turubanova et al. 2023, Viana-Soto and Senf 2025 and Viana-Soto et al. 2026). Letters in each point indicate the country by ISO2-Code. The period of analysis is constrained to 2001 to 2018, which is covered by all datasets. Bias is quantified as the mean signed deviation.

5 Conclusion and future use

We here present an up-to-date database on forest disturbance occurrence across 35,000 locations in Europe, covering the years 1985 to 2023. Our database provides the most comprehensive and reliable source on tree cover change at the European level, allowing for robust estimation of disturbance area and trends, and serving as benchmark for future studies. Our application example shows that disturbance rates are highly variable between countries in Europe, but that rates have increased in most countries, with highest disturbance rates observed in the most recent years. Besides our application example, our data can be used for map validation, comparing disturbances mapped from satellite data against our manual interpretation. Doing so will help in understanding uncertainties in global and regional forest disturbance maps, hopefully reducing bias in estimates of disturbance rates and trends across Europe.

https://doi.org/10.5194/essd-2026-422
Preprint. Discussion started: 7 September 2026

Open Access Earth System Science Data Discussions

Code and data availability

The database including raw data are available from https://doi.org/10.5281/zenodo.22101910 (Senf et al., 2026). All R scripts for processing the raw data into the final database are also available in the repository. The R scripts for the application example can be accessed here: https://gist.github.com/corneliussenf/27327f0f99e33664b1bcec738af27a66.

Author contributions

CS, AVS and KK conceptualized the study. FWG and AVS curated the data and supervised investigations. AKB, VE, PE, JH, MH, JH, AH, NBM, AO, MR and KV performed all investigations. CS developed the methodology and conducted the formal analysis, with contributions from AVS and KK. BJ provided software. CS wrote the original draft. All authors reviewed and edited the final draft. CS and AVS acquired the funding.

Competing interests

The authors declare no competing interests.

Disclaimer

Copernicus Publications remains neutral with regard to jurisdictional claims made in the text, published maps, institutional affiliations, or any other geographical representation in this paper. While Copernicus Publications makes every effort to include appropriate place names, the final responsibility lies with the authors. Views expressed in the text are those of the authors and do not necessarily reflect the views of the publisher.

Financial support

We acknowledge funding from the European Forest Institute (G-06-2023-1), Horizon Europe though ForestPaths (101056755), the European Space Agency through Climate-Space RECCAP2 (4000144908/24/I-LR), and Germany's Federal Ministry of Education and Research through AI4Forest (01IS23025C).

Review statement

The review statement will be added by Copernicus Publications listing the handling editor as well as all contributing referees according to their status anonymous or identified.

References

Breidenbach, J., Granhus, A., Hylen, G., Eriksen, R., and Astrup, R.: A century of National Forest Inventory in Norway – informing past, present, and future decisions, Forest Ecosystems, 7, 46, https://doi.org/10.1186/s40663-020-00261-0, 2020.

Carpenter, B., Gelman, A., Hoffman, M. D., Lee, D., Goodrich, B., Betancourt, M., Brubaker, M., Guo, J., Li, P., and Riddell, A.: Stan: A Probabilistic Programming Language, Journal of Statistical Software, 76, 1–32, https://doi.org/10.18637/jss.v076.i01, 2017.

Ceccherini, G., Duveiller, G., Grassi, G., Lemoine, G., Avitabile, V., Pilli, R., and Cescatti, A.: Abrupt increase in harvested forest area over Europe after 2015, Nature, 583, 72–77, https://doi.org/10.1038/s41586-020-2438-y, 2020.

Ceccherini, G., Duveiller, G., Grassi, G., Lemoine, G., Avitabile, V., Pilli, R., and Cescatti, A.: Potentials and limitations of NFIs and remote sensing in the assessment of harvest rates: a reply to Breidenbach et al., Annals of Forest Science, 79, 31, https://doi.org/10.1186/s13595-022-01150-y, 2022.

Cohen, W., Healey, S., Yang, Z., Stehman, S., Brewer, C., Brooks, E., Gorelick, N., Huang, C., Hughes, M., Kennedy, R., Loveland, T., Moisen, G., Schroeder, T., Vogelmann, J., Woodcock, C., Yang, L., and Zhu, Z.: How Similar Are Forest Disturbance Maps Derived from Different Landsat Time Series Algorithms?, Forests, 8, 98, https://doi.org/10.3390/f8040098, 2017.

Cohen, W. B., Yang, Z., and Kennedy, R.: Detecting trends in forest disturbance and recovery using yearly Landsat time series: 2. TimeSync — Tools for calibration and validation, Remote Sensing of Environment, 114, 2911–2924, https://doi.org/10.1016/j.rse.2010.07.010, 2010.

Cohen, W. B., Yang, Z. Q., Stehman, S. V., Schroeder, T. A., Bell, D. M., Masek, J. G., Huang, C. Q., and Meigs, G. W.: Forest disturbance across the conterminous United States from 1985-2012: The emerging dominance of forest decline, Forest Ecology and Management, 360, 242–252, https://doi.org/10.1016/j.foreco.2015.10.042, 2016.

Fassnacht, F. E., Latifi, H., Ghosh, A., Joshi, P. K., and Koch, B.: Assessing the potential of hyperspectral imagery to map bark beetle-induced tree mortality, Remote Sensing of Environment, 140, 533–548, https://doi.org/10.1016/j.rse.2013.09.014, 2014.

Francini, S., Hermosilla, T., Coops, N. C., Wulder, M. A., White, J. C., and Chirici, G.: An assessment approach for pixel-based image composites, ISPRS Journal of Photogrammetry and Remote Sensing, 202, 1–12, https://doi.org/10.1016/j.isprsjprs.2023.06.002, 2023.

Frantz, D.: FORCE—Landsat + Sentinel-2 Analysis Ready Data and Beyond, Remote Sensing, 11, 1124, https://doi.org/10.3390/rs11091124, 2019.

Frantz, D., Rufin, P., Janz, A., Ernst, S., Pflugmacher, D., Schug, F., and Hostert, P.: Understanding the robustness of spectral-temporal metrics across the global Landsat archive from 1984 to 2019 – a quantitative evaluation, Remote Sensing of Environment, 298, 113823, https://doi.org/10.1016/j.rse.2023.113823, 2023.

Gorelick, N., Hancher, M., Dixon, M., Ilyushchenko, S., Thau, D., and Moore, R.: Google Earth Engine: Planetary-scale geospatial analysis for everyone, Remote Sensing of Environment, 202, 18–27, https://doi.org/10.1016/j.rse.2017.06.031, 2017.

Griffiths, P., Van der Linden, S., Kuemmerle, T., and Hostert, P.: A pixel-based Landsat compositing algorithm for large area land cover mapping, IEEE Journal of Selected Topics in Applied Earth Observations and Remote Sensing, 6, 2088–2101, 2013.

Hansen, M. C., Potapov, P. V., Moore, R., Hancher, M., Turubanova, S. A., Tyukavina, A., Thau, D., Stehman, S. V., Goetz, S. J., Loveland, T. R., Kommareddy, A., Egorov, A., Chini, L., Justice, C. O., and Townshend, J. R.: High-resolution global maps of 21st-century forest cover change, Science, 342, 850–3, https://doi.org/10.1126/science.1244693, 2013.

Hermosilla, T., Wulder, M. A., White, J. C., Coops, N. C., and Hobart, G. W.: Regional detection, characterization, and attribution of annual forest change from 1984 to 2012 using Landsat-derived time-series metrics, Remote Sensing of Environment, 170, 121–132, https://doi.org/10.1016/j.rse.2015.09.004, 2015.

Jakimow, B., van der Linden, S., Thiel, F., Frantz, D., and Hostert, P.: Visualizing and labeling dense multi-sensor earth observation time series: The EO Time Series Viewer, Environmental Modelling & Software, 125, 104631, https://doi.org/10.1016/j.envsoft.2020.104631, 2020.

Lechner, A. M., Foody, G. M., and Boyd, D. S.: Applications in Remote Sensing to Forest Ecology and Management, One Earth, 2, 405–412, https://doi.org/10.1016/j.oneear.2020.05.001, 2020.

https://doi.org/10.5194/essd-2026-422
Preprint. Discussion started: 7 September 2026

Lecina-Diaz, J., Senf, C., Grünig, M., and Seidl, R.: Ecosystem services at risk from disturbance in Europe’s forests, Global Change Biology, 30, https://doi.org/10.1111/gcb.17242, 2024.

Lerink, B. J. W., Schelhaas, M.-J., Schreiber, R., Aurenhammer, P., Kies, U., Vuillermoz, M., Ruch, P., Pupin, C., Kitching, A., Kerr, G., Sing, L., Calvert, A., Ní Dhubháin, Á., Nieuwenhuis, M., Vayreda, J., Reumerman, P., Gustavsonn, G., Jakobsson, R., Little, D., Thivolle-Cazat, A., Orazio, C., and Nabuurs, G.-J.: How much wood can we expect from European forests in the near future?, Forestry (Lond), 96, 434–447, https://doi.org/10.1093/forestry/cpad009, 2023.

McDowell, N. G., Coops, N. C., Beck, P. S., Chambers, J. Q., Gangodagamage, C., Hicke, J. A., Huang, C. Y., Kennedy, R., Krofcheck, D. J., Litvak, M., Meddens, A. J., Muss, J., Negron-Juarez, R., Peng, C., Schwantes, A. M., Swenson, J. J., Vernon, L. J., Williams, A. P., Xu, C., Zhao, M., Running, S. W., and Allen, C. D.: Global satellite monitoring of climate-induced vegetation disturbances, Trends Plant Sci, 20, 114–23, https://doi.org/10.1016/j.tplants.2014.10.008, 2015.

Migliavacca, M., Grassi, G., Bastos, A., Ceccherini, G., Ciais, P., Janssens-Maenhout, G., Lugato, E., Mahecha, M. D., Novick, K. A., Peñuelas, J., Pilli, R., Reichstein, M., Avitabile, V., Beck, P. S. A., Barredo, J. I., Forzieri, G., Herold, M., Korosuo, A., Mansuy, N., Mubareka, S., Orth, R., Rougieux, P., and Cescatti, A.: Securing the forest carbon sink for the European Union’s climate ambition, Nature, 643, 1203–1213, https://doi.org/10.1038/s41586-025-08967-3, 2025.

Mohr, J. S., Bastit, F., Grünig, M., Knoke, T., Rammer, W., Senf, C., Thom, D., and Seidl, R.: Rising cost of disturbances for forestry in Europe under climate change, Nat. Clim. Chang., 1–6, https://doi.org/10.1038/s41558-025-02408-9, 2025.

Olofsson, P., Foody, G. M., Stehman, S. V., and Woodcock, C. E.: Making better use of accuracy data in land change studies: Estimating accuracy and area and quantifying uncertainty using stratified estimation, Remote Sensing of Environment, 129, 122–131, https://doi.org/10.1016/j.rse.2012.10.031, 2013.

Olofsson, P., Foody, G. M., Herold, M., Stehman, S. V., Woodcock, C. E., and Wulder, M. A.: Good practices for estimating area and assessing accuracy of land change, Remote Sensing of Environment, 148, 42–57, https://doi.org/10.1016/j.rse.2014.02.015, 2014.

Palahí, M., Valbuena, R., Senf, C., Acil, N., Pugh, T. A. M., Sadler, J., Seidl, R., Potapov, P., Gardiner, B., Hetemäki, L., Chirici, G., Francini, S., Hlásny, T., Lerink, B. J. W., Olsson, H., González Olabarria, J. R., Ascoli, D., Asikainen, A., Bauhus, J., Berndes, G., Donis, J., Fridman, J., Hanewinkel, M., Jactel, H., Lindner, M., Marchetti, M., Marušák, R., Sheil, D., Tomé, M., Trasobares, A., Verkerk, P. J., Korhonen, M., and Nabuurs, G.-J.: Concerns about reported harvests in European forests, Nature, 592, E15–E17, https://doi.org/10.1038/s41586-021-03292-x, 2021.

Patacca, M., Lindner, M., Lucas-Borja, M. E., Cordonnier, T., Fidej, G., Gardiner, B., Hauf, Y., Jasinevičius, G., Labonne, S., Linkevičius, E., Mahnken, M., Milanovic, S., Nabuurs, G.-J., Nagel, T. A., Nikinmaa, L., Panyatov, M., Bercak, R., Seidl, R., Ostrogović Sever, M. Z., Socha, J., Thom, D., Vuletic, D., Zudin, S., and Schelhaas, M.-J.: Significant increase in natural disturbance impacts on European forests since 1950, Global Change Biology, 29, 1359–1376, https://doi.org/10.1111/gcb.16531, 2023.

Pickens, A. H., Hansen, M. C., Hancher, M., Stehman, S. V., Tyukavina, A., Potapov, P., Marroquin, B., and Sherani, Z.: Mapping and sampling to characterize global inland water dynamics from 1999 to 2018 with full Landsat time-series, Remote Sensing of Environment, 243, 111792, https://doi.org/10.1016/j.rse.2020.111792, 2020.

Roy, D. P., Kovalskyy, V., Zhang, H. K., Vermote, E. F., Yan, L., Kumar, S. S., and Egorov, A.: Characterization of Landsat-7 to Landsat-8 reflective wavelength and normalized difference vegetation index continuity, Remote Sensing of Environment, 185, 57–70, https://doi.org/10.1016/j.rse.2015.12.024, 2016.

Seidl, R. and Senf, C.: Changes in planned and unplanned canopy openings are linked in Europe’s forests, Nat Commun, 15, 4741, https://doi.org/10.1038/s41467-024-49116-0, 2024.

Seidl, R., Schelhaas, M.-J., and Lexer, M. J.: Unraveling the drivers of intensifying forest disturbance regimes in Europe, Global Change Biology, 17, 2842–2852, https://doi.org/10.1111/j.1365-2486.2011.02452.x, 2011.

Seidl, R., Schelhaas, M. J., Rammer, W., and Verkerk, P. J.: Increasing forest disturbances in Europe and their impact on carbon storage, Nature Climate Change, 4, 806–810, https://doi.org/10.1038/nclimate2318, 2014.

Senf, C.: Seeing the System from Above: The Use and Potential of Remote Sensing for Studying Ecosystem Dynamics, Ecosystems, https://doi.org/10.1007/s10021-022-00777-2, 2022.

Senf, C. and Seidl, R.: Mapping the forest disturbance regimes of Europe, Nat Sustain, 4, 63–70, https://doi.org/10.1038/s41893-020-00609-y, 2021.

Senf, C., Pflugmacher, D., Zhiqiang, Y., Sebald, J., Knorn, J., Neumann, M., Hostert, P., and Seidl, R.: Canopy mortality has doubled in Europe’s temperate forests over the last three decades, Nat Commun, 9, 4978, https://doi.org/10.1038/s41467-018-

07539-6, 2018.

Senf, C., Buras, A., Zang, C. S., Rammig, A., and Seidl, R.: Excess forest mortality is consistently linked to drought across Europe, Nature Communications, 11, 6200, https://doi.org/10.1038/s41467-020-19924-1, 2020.

Senf, C., Sebald, J., and Seidl, R.: Increasing canopy mortality affects the future demographic structure of Europe's forests, One Earth, 4, 749–755, https://doi.org/10.1016/j.oneear.2021.04.008, 2021.

Senf, C., Esquivel-Muelbert, A., Pugh, T. A. M., Anderegg, W. R. L., Anderson-Teixeira, K. J., Arellano, G., Beloiu Schwenke, M., Bentz, B. J., Boehmer, H. J., Bond-Lamberty, B., Bordin, K. M., Brearley, F. Q., Bussotti, F., Cailleret, M., Camarero, J. J., Chirici, G., Costa, F. R. C., Dalagnol, R., Davi, H., Davies, S. J., Delzon, S., Dhakal, B. P., Ferreira de Lima, R. A., Ferretti, M., Fontaine, J. B., Garbarino, M., de Gasper, A. L., Gessler, A., Gilbert, G. S., Godlee, J. L., Gonçalves, F. M. P., Govaere, L., Gutiérrez, A. G., Cardozo, E. G., Hammond, W. M., Hartmann, H., Hobi, M. L., Holz, A., Homeier, J., Hovenden, M. J., Huang, C.-Y., Hérault, B., Jackson, T., Jucker, T., Jump, A. S., Junttila, S., Kattenborn, T., Klipel, J., Kotowska, M. M., Král, K., La Porta, N., Lopez-Toledo, L., López-Camacho, R., Maeda, E. E., Mallol Díaz, J., Martin, E. H., Martínez-Vilalta, J., McDowell, N., Moonlight, P. W., Mori, A. S., Muda, M. A., Mund, J.-P., Muscarella, R., Méndez-Toribio, M., Müller, S. C., Nagel, T. A., Neagu, S., Nock, C. A., Nsanyi Sainge, M., O'Brien, M. J., Peñuelas, J., Perry, G. L. W., Phillips, O. L., Posada, J. M., Rodrigues, R. R., Roman, A., Rousseau, G. X., Ruehr, N. K., Ruiz-Benito, P., Ruthrof, K. X., Salas-Eljatib, C., Sanders, T., Scarton Bergamin, R., Scharnweber, T., Schelhaas, M.-J., Schuldt, B., Schwarz, S., Seidl, R., Shorohova, E., Silva, A. C., Sioen, G., Socha, J., Stereńczak, K., Stillhard, J., Stojanović, D. B., Suvanto, S., Svoboda, M., Sánchez-Pinillos, M., Tanentzap, A. J., et al.: Towards a global understanding of tree mortality, New Phytologist, 245, 2377–2392, https://doi.org/10.1111/nph.20407, 2025.

Senf, C., Wieland-Glasmann, F., Kowalski, K., Jakimow, B., Behrens, A.-K., Egger, V., Ermert, P., Hänle, J., Hanzing, M., Heinrich, J., Hostlowsky, A., Mauer, N. B., Onay, A., Rachfahl, M., Voggeneder, K., and Viana-Soto, A.: Database of forest disturbance reference samples for Europe (2), https://doi.org/10.5281/zenodo.22101910, 2026.

Stehman, S. V.: Practical Implications of Design-Based Sampling Inference for Thematic Map Accuracy Assessment, Remote Sensing of Environment, 72, 35–45, https://doi.org/10.1016/S0034-4257(99)00090-5, 2000.

Stehman, S. V.: Sampling designs for accuracy assessment of land cover, International Journal of Remote Sensing, 30, 5243–5272, https://doi.org/10.1080/01431160903131000, 2009.

Stehman, S. V. and Foody, G. M.: Key issues in rigorous accuracy assessment of land cover products, Remote Sensing of Environment, 231, 111199, https://doi.org/10.1016/j.rse.2019.05.018, 2019.

Suvanto, S., Esquivel Muelbert, A., Schelhaas, M.-J., Astigarraga, J., Astrup, R., Cienciala, E., Fridman, J., Henttonen, H., Kunstler, G., Kändler, G., König, L., Ruiz-Benito, P., Senf, C., Stadelmann, G., Starcevic, A., Talarczyk, A., Zavala, M., and Pugh, T.: Understanding Europe's forest harvesting regimes, https://doi.org/10.31223/X5910J, 2023.

Turubanova, S., Potapov, P., Hansen, M. C., Li, X., Tyukavina, A., Pickens, A. H., Hernandez-Serna, A., Arranz, A. P., Guerra-Hernandez, J., Senf, C., Häme, T., Valbuena, R., Eklundh, L., Brovkina, O., Navrátilová, B., Novotný, J., Harris, N., and Stolle, F.: Tree canopy extent and height change in Europe, 2001–2021, quantified using Landsat data archive, Remote Sensing of Environment, 298, 113797, https://doi.org/10.1016/j.rse.2023.113797, 2023.

Tyukavina, A., Stehman, S. V., Pickens, A. H., Potapov, P., and Hansen, M. C.: Practical global sampling methods for estimating area and map accuracy of land cover and change, Remote Sensing of Environment, 324, 114714, https://doi.org/10.1016/j.rse.2025.114714, 2025.

Viana-Soto, A. and Senf, C.: The European Forest Disturbance Atlas: a forest disturbance monitoring system using the Landsat archive, Earth Syst. Sci. Data, 17, 2373–2404, https://doi.org/10.5194/essd-17-2373-2025, 2025.

Wernick, I. K., Ciais, P., Fridman, J., Högberg, P., Korhonen, K. T., Nordin, A., and Kauppi, P. E.: Quantifying forest change in the European Union, Nature, 592, E13–E14, https://doi.org/10.1038/s41586-021-03293-w, 2021.

Zhu, Z. and Woodcock, C. E.: Object-based cloud and cloud shadow detection in Landsat imagery, Remote Sensing of Environment, 118, 83–94, https://doi.org/10.1016/j.rse.2011.10.028, 2012.